

Utilization of Drinking Water Treatment Plant Sludge with High Calcium Fly Ash as Geopolymer Precursor for Paving Cement-free Bricks

LeenaVachasiddha,^{a,b,©}, ShaliniTandon^b, Rakesh Kumar^c

^a - Academy of Scientific and Innovative Research (AcSIR), Ghaziabad, 201002, India

^b - CSIR-NEERI, Mumbai Research & Innovation Centre. 89-B Dr. A.B. Road Worli, Mumbai 400 018, India

^c - Council of Scientific & Industrial Research (CSIR), 2 Rafi Marg AnusandhanBhavan, Delhi 110001, India

©Corresponding author: leena.vachasiddha@gmail.com

Submitted:26January 2023

Revised:17 February 2023

Accepted: 27February 2023

Abstract: The construction industry is facing challenges in terms of sustainability as a lot of virgin natural materials are utilized every year. On the one hand, construction needs more material, on the other, waste material from anthropogenic activities produces large volumes of byproducts like fly ash and water treatment plant sludge that require proper disposal. Two waste by-products namely, drinking water treatment plant sludge of Bhandup Water Complex of Brihanmumbai Municipal Corporation and high calcium fly ash from Trombay Thermal Power Plant have been used to synthesize geopolymers. A mixture of Sodium silicate and sodium hydroxide solutions was used as the liquid alkaline activating solution. Influence of various factors such as molar ratios of $\text{SiO}_2:\text{Na}_2\text{O}$ of activating solution, $\text{SiO}_2:\text{Al}_2\text{O}_3$ of the mix, $\text{Na}:\text{Al}$ of the mix, curing temperature, and time were studied. Fourier Transform Infrared Spectroscopy (FTIR) and Scanning Electron Microscopy (SEM) tools were used to understand the influence of these factors on geopolymer specimens. Statistically, molar ratios of Na/Al affect the geopolymerization process as reflected in the measurement of the compressive strength of the samples. The results obtained demonstrate the feasibility of recycling aluminosilicate-rich wastes which are primarily disposed in the open with serious environmental damage. Results indicate a very promising area for recycling and a useful perspective for their application.

Keywords: Geopolymer, drinking water sludge, high calcium fly ash, compressive strength, molar ratios, cement-free bricks

I. INTRODUCTION

Urbanization, population growth, and improved standard of living have caused increased stress on water utilities to produce more drinking water than before (Ahmad et al., 2017). A typical drinking water treatment process consists of coagulation-flocculation, sedimentation, filtration, and chlorination. This process also yields another by-product called drinking water sludge also called alum sludge, as alum is one the most popularly used coagulants. It is estimated that around 10,000 tonnes of drinking water sludge is produced every day on a global scale (Babatunde & Zhao, 2007). The most common disposal methods for sludge include releasing it in open drains, returning it to raw water sources, and landfilling. However, increasing costs of disposal and lack of space have made landfilling an expensive option. For instance, disposal costs of sludge in the UK exceed £5.5 million

(Keeley et al., 2014) annually (for about 182,000 tonnes of dry solids in the year 2000) while in the Netherlands it is around £30-40 million pounds (Horth H, 1994). The drinking water treatment sludge can be also classified as a high volume and non-hazardous waste which can be turned into a useful alternative like filler material or precursor in the construction industry as they are rich in silica and alumina.

Water treatment plant (WTP) sludge use has been explored: as a partial replacement to clay in brick making, as a partial replacement to cement, in making lightweight aggregates (C. H. Huang & Wang, 2013; Sales et al., 2011), as controlled low-strength material (CLSM) (Fang et al., 2019; Tang & Cheng, 2019) and as geopolymers. Some researchers have substituted up to 20% of clay with WTP sludge to obtain bricks with compressive strength $> 100 \text{ kg/cm}^2$ (C. Huang et

al., 2001) while others have explored firing the WTP sludge-clay specimens at lower temperatures i.e. 950°C only to obtain second or third-degree acceptable bricks (C. Huang et al., 2005). The presence of iron oxide in the sludge contributed to darker pigment in the product and also resulted in a 16% increase in the compressive strength of bricks (Kiziničević et al., 2013). Ceramic bricks have been made by substituting up to 30% weight water treatment plant sludge and the specimens obtained were similar to control brick made of pure clay (Teixeira et al., 2011). It was also observed that the addition of WTP sludge to clay affected the quality of the ceramics and in some cases worsened it (Monteiro et al., 2008). Successful replacement of sludge as a partial replacement in cement production showed an increase in compressive strength with no leaching of heavy metals (Chen et al., 2010; El-Didamony et al., 2014; Pan et al., 2004). Recently, sludge has also been explored in making geopolymer specimens obtaining compressive strength of more than 20 MPa and going beyond 50 MPa in some cases (Ferone et al., 2019; Messina et al., 2017; Santos et al., 2019; Suksiripattanapong, Horpibulsuk, Boongrasan, et al., 2015).

Fly ash is one of the most commonly produced high-volume wastes in the world that is derived from coal-fired thermal power plants (Mohapatra & Rao, 2001). It is also the most popularly used supplementary additive to cement often up to 25-30%. These are mainly composed of aluminosilicate compounds along with some metals and calcium oxides (Iribarne et al., 2001). Low calcium fly ash has been used widely in concrete and geopolymer as they exhibit good performance (Yao et al., 2015) while high calcium fly ash may contribute to premature distress in concrete due to the formation of ettringite (D, 1997)(Tishmack et al., 1999).

Globally, the geopolymerization process has recently started gaining importance as it has low CO₂ emission, high performance and durability, fire resistance, corrosion resistance, and low energy consumption (Cong et al., 2021). Geopolymers consist of a network of mineral molecules bonded by covalent bonds to form a condensed structure at low temperatures typically around 100°C (Davidovits, 2017). The key components in the geopolymerization process include alkaline activating binder solution, precursors rich in silica and alumina, and filler materials – viz. fine and coarse aggregate. The silica and alumina from the precursor materials dissolve in the alkaline activating solution at room temperature or higher temperature to form an amorphous phase consisting of a three-dimensional silico-aluminate structure (Ren et al., 2017). There are currently no standards for geopolymer concrete globally. Different synthesis processes and methodologies have been applied by various researchers to achieve their objectives. For example, some have used drinking water treatment sludge as aggregates (Horpibulsuk et al., 2016; Suksiripattanapong, Horpibulsuk, Boongrasan, et al., 2015) while others have used them as precursors (Messina et al., 2017; Waijarean et al., 2014). Another highlight is that most of these sludges have been subjected to calcination to improve their pozzolanic activity and performance (Messina et al., 2017; Nimwinya et al., 2016; Tantawy, 2015). Without calcination, the sludge showed delayed setting time, low

compressive strength, and workability (Waijarean et al., 2014). The majority of the work has been done using alkaline sodium-based silicate solutions as they promote better dissolution for the aluminosilicates (Davidovits et al., 2008). Geopolymers with low calcium fly ash have been used by many (Mudgal et al., 2021; Suksiripattanapong, Horpibulsuk, Chanprasert, et al., 2015) to form geopolymer specimens. However, some findings report that better strength is achieved with high calcium fly ash as the formation of Calcium Silica Hydrate (CASH) gels in addition to Sodium Aluminosilicate Hydrate (NASH) gels, and the presence of calcium also initiates early setting time (Davidovits et al., 2008; Mahmoodi et al., 2020).

This study introduces a novel approach wherein calcined drinking water sludge, in combination with high calcium fly ash, is proposed to produce cement-free, water-free geopolymeric mortar and concrete. This method follows specific pre-determined molar ratios of Na/Al, SiO₂:Al₂O₃, Na:Al, and a combination of curing conditions. The present work brings out findings on the characterization of drinking water sludge and high calcium fly ash to assess the impact of calcination on geopolymers. It also determines the optimal molar ratios with sludge and fly ash through the testing of geopolymer pastes and concrete from mechanical and microstructural perspectives.

Furthermore, the study evaluates the properties of the product through proximate and ultimate analysis of raw materials, as well as other relevant properties of hardened geopolymers including density, porosity, water absorption, and compressive strength. Detailed microstructural analysis utilizing Scanning Electron Microscopy (SEM), Fourier Transform Infrared (FTIR), and Toxicity Characteristic Leaching Procedure (TCLP) is conducted to characterize and elucidate the acquired properties in the geopolymeric specimens tested under the study.

The rationale behind this research stems from the necessity to responsibly manage the growing quantities of drinking water sludge and fly ash, which can find application in various construction-related activities. Additionally, the study leads to the conclusion that it's advantageous to upcycle wastes for developing cement-free products. It also encourages the exploration of calcined pozzolanic materials from diverse sources to meet the escalating construction demands in the country.

II. MATERIAL & METHODS

Raw Material collection

The water treatment plant sludge was collected from the centrifuge outlet of the Bhandup Water Complex of MCGM, Bhandup, Mumbai while the high calcium fly ash was collected from fly ash silos from TATA Trombay Thermal Power Plant, Mumbai, India. The sludge was collected during the pre-monsoon season. The Bhandup Water Complex is the largest drinking water treatment plant in Asia and supplies drinking water to the tune of 2900 MLD through conventional

treatment processes of coagulation, flocculation, and rapid sand filtration, using Polyaluminium Chloride (PAC) as the main coagulant. The Bhandup water complex produces about 196 tons/month of sludge in the dry season and about 600 tons/month in the wet season. The sludge produced is stored in the lagoons within the water complex and some of it is sent to dumping ground as cover soil. The Trombay thermal power plant generates 930MW of electricity and about 2700 MT of fly ash every month.

Sample preparation, calcination, and characterization

Sample preparation: The sludge was sun-dried to evaporate the moisture and oven-dried at 105°C before milling in the ball mill with a ball-to-sludge ratio of 6:1 at 75 rpm for 2 hours, sieved with a 40-micron mesh size to get a homogenous sample. Moisture-free fly ash was used in the same condition as it was collected.

Calcination of sludge: Calcination of the sludge samples was carried out in a laboratory muffle furnace. The muffle furnace achieved the desired temperature at 10°C/min ramping rate. The ball-milled sludge was spread in thin layers on ceramic crucibles at a temperature range of 500°C up to 800°C for one hour respectively. The samples were allowed to cool gradually overnight without any heat shocks and transferred into a desiccator before storage. The liquid alkaline activating solution was a blend of Sodium Silicate Solution (molar ratio (R) of $\text{SiO}_2:\text{Na}_2\text{O}$ –3.39) supplied by Lobachemie and Sodium Hydroxide pellets (purity 98%) supplied by Merck, India. The commercial sodium silicate solution consisted of 27.89% SiO_2 , 8.47% Na_2O , and 63.64% H_2O , by weight.

Characterization of raw materials: Characterization of the sludge, calcined sludge, and fly ash was done using elemental, mineralogical, and spectroscopic analysis.

The proximate analysis (moisture, volatile matter & ash content) of the samples was carried out in the laboratory following the procedures as given in APHA (2540 G) and the ultimate analysis was tested by CHNS analyzer by LECO Model 628. Density, specific gravity, and particle size (using a hydrometer) were carried out in the laboratory as per IS CODE 2720 guidelines. pH of the samples was tested using a handheld pH meter by Hanna (Model H18424 Portable pH meter). Pozzolanicity of the materials was conducted with the Modified Chapelle Test as given in French Norm NF P 18-513. The elemental, mineral, and spectroscopic analysis of materials was done using sophisticated instrumentation techniques such as XRF, XRD, SEM, FTIR, and TOC. X-ray fluorescence (XRF) of the samples was done via model Rigaku Primus-III to estimate the elemental composition of the raw materials in the form of metal oxides. X-ray diffraction (XRD) analysis was carried out using Smart Lab SE by Rigaku Powder XRD ver. 4.01.0 (K β filter 1D for Cu, 40 kV, 45 mA, 2 θ range from 10°~ 80°, step width 0.01°, 0.5° slit width). SEM analysis was carried out using the TESCAN model VEGA 3 XMU. Total Organic Carbon was estimated by Shimadzu TOC analyzer model TOC-VCPH. FTIR was estimated by Vertex 80 FTIR System Bruker, Germany in the range of 400 to 4000 cm^{-1} .

Moulds: The geopolymer specimens of sizes - 50×50×50 mm and 100×100×100 mm were made of cast iron and steel moulds. Moulds were cleaned and brushed internally with black oil for easy removal of specimens upon curing. Previously, plastic film and thin paper sheets were tried as releasing agents, however, none of them released the specimens easily and led to the cracking of the specimens while demoulding esp. at the edges.

Mix design for paste, mortars, and precast elements

Water treatment plant sludge was used in two forms – raw uncalcined and calcined form. Calcination of sludge was carried out in a temperature range of 500°C up to 800°C for one hour. This was done in the crucible by evenly spreading the sludge up to 2-3 mm thickness before placing it in the muffle furnace.

Initially, high calcium fly ash and raw water treatment plant sludge were used in combination with an alkaline activating solution to form binder cubes with different ratios. In Batch I, three different pastes were prepared as given in **Table 1**.

The pastes were mixed using a Hobart mixer in the laboratory. The dry powders were mixed at low speed for 3 mins and the alkaline activating solution was added slowly for about 30 seconds. After mixing for 2 mins at medium speed, the edges were scraped with a spatula for the last 1 min at high speed. The paste was cast in a 50×50×50 mm sized cast iron mould that was oiled from the inside for better release of the specimen. The samples were cured at two different conditions – ambient room temperature (~38°C) and in the oven at 60°C for 24 hrs. They were first kept for curing while being in the mould for 24 hrs. and then after drying were demoulded. Mortar with the same composition was prepared with sand consisting of 50% of the total solids by weight. The sand used was river sand with a grain size of 0-4.75 mm. All specimens were cast in triplicates for each mix. The geopolymer mortar specimens were cured at ambient room temperature and 60°C in the oven for 24 hrs. Demoulding was done post-initial curing and samples were kept in their respective curing conditions until the 28th day. Compressive strength was tested on the 28th day at the structural engineering department of Veermata Jijabai Technological Institute (VJTI), Mumbai, India.

Based on the results obtained in Table 1, the experimental design was modified based on the molar ratio of $\text{SiO}_2:\text{Al}_2\text{O}_3$ and $\text{Na}:\text{Al}$, and new batches of geopolymer mortar and concrete were cast. The composition of this Batch II is given in **Table 2**. Calcined sludge was also used in this batch. The sand used was river sand with a grain size of 0-4.75 mm and coarse aggregate used were natural aggregates with grain size between 5–10 mm. All specimens were cast in triplicates for each mix.

The mixing procedure for mortar (M1-M4) followed was similar except for the addition of sodium hydroxide and precursor powders first for 5 mins and then adding sodium silicate solution slowly to the mix. The sand was added in the ratio of 1:4 (precursor to sand on a weight basis) to the mix.

The specimens were covered on top with a plastic bag before hardening. The geopolymer concrete (M5-M6) was made similarly with a single modification of mixing the components

of the alkaline activating solution 24 hr. before use. The results and observations are discussed in section 3.0.

TABLE 1
Compositions of Geopolymer Pastes and Mortars

| Sample Code | Sample Composition (By Vol.) | SiO ₂ (gms) | Al ₂ O ₃ (gms) | Na ₂ O (gms) | SiO ₂ :Al ₂ O ₃ Molar Ratio Of Mix | SiO ₂ :Na ₂ O Molar Ratio Of Mix | Na ₂ O:Al ₂ O ₃ Molar Ratio Of Mix | Sodium Silicate To Sodium Hydroxide Ratio (By Vol.) |
|-------------|----------------------------------|------------------------|--------------------------------------|-------------------------|---|--|---|---|
| G1 Paste | 50 Raw Sludge/50 Fly Ash | 123.17 | 56.51 | 33.99 | 3.70 | 3.59 | 1.03 | 50 SS/50 SH |
| G2 Paste | 70 Raw Sludge/30 Fly Ash | 108.37 | 50.67 | 11.78 | 3.68 | 5.25 | 0.70 | 70 SS/30 SH |
| G3 Paste | 30 Raw Sludge/70 Fly Ash | 122.89 | 58.14 | 37.93 | 3.59 | 3.18 | 1.13 | 30 SS/70 SH |
| G4 Mortar | 50 Raw Sludge/50 Fly Ash + Sand* | 102.38 | 45.53 | 31.83 | 3.82 | 3.20 | 1.19 | 50 SS/50 SH |
| G5 Mortar | 70 Raw Sludge/30 Fly Ash + Sand* | 122.73 | 54.18 | 25.03 | 3.84 | 4.83 | 0.80 | 70 SS/30 SH |
| G6 Mortar | 30 Raw Sludge/70 Fly Ash + Sand* | 102.66 | 48.31 | 33.10 | 3.92 | 4.45 | 0.88 | 30 SS/70 SH |

Note: The sand added was 50% of the total precursor solids, no extra water was added to the mortar

TABLE 2
Composition of Geopolymer Mortars and Concrete with varying SiO₂:Al₂O₃ ratios

| Sample Code | Sample Composition | SiO ₂ :Al ₂ O ₃ Molar Ratio of Mix | SiO ₂ :Na ₂ O Molar Ratio of Mix | Na ₂ O:Al ₂ O ₃ Molar Ratio of Mix | Binder: Aggregate: Coarse Aggregate Ratio (By Weight) |
|-------------|---|---|--|---|---|
| M1 | Fly Ash, Raw Sludge, Sand, Alkaline Activating Solution | 3.18 | 1.51 | 2.11 | 1: 4: 0 |
| M2 | Fly Ash, Raw Sludge, Sand, Alkaline Activating Solution | 3.90 | 1.37 | 2.85 | 1: 4: 0 |
| M3 | Fly Ash, Raw Sludge, Sand, Alkaline Activating Solution | 5.16 | 3.25 | 1.59 | 1: 4: 0 |
| M4 | Fly Ash, Raw Sludge, Sand, Alkaline Activating Solution | 6.78 | 4.55 | 1.49 | 1: 4: 0 |
| M5 | Fly Ash, Raw Sludge, Sand, Coarse Aggregates, Alkaline Activating Solution | 4.01 | 4.41 | 0.91 | 1: 1.5: 3 |
| M6 | Fly Ash, Calcined Sludge (At 600°C For 1 Hour), Sand, Coarse Aggregates, Alkaline Activating Solution | 4.01 | 4.41 | 0.91 | 1: 1.5: 3 |

Note: Alkaline activators – mix of commercial Sodium silicate solution, and 10M Sodium hydroxide solution (were added such that the molar ratio of the mix was achieved as desired)

To make chemically balanced geopolymers, the methodology of mixing and molar ratio of Na₂O:Al₂O₃ of the total mix and SiO₂:Na₂O ratio of alkaline activating solution were investigated along with varying curing conditions and time. The outcomes from Batch II were incorporated and improved to understand the influence of variables on the compressive strength of the geopolymers. The details of Batch III trial mixes are given in **Table 3**.

In batch III, the process of mixing of the components and their making was improvised. The alkaline activating solution

was mixed with geopolymer precursor with the help of an overhead stirrer at about 350 rpm for 10-15 mins till homogenised. The mix was kept in an incubator at 20°C for 1 hour to age. Coarse aggregate with grain size > 5mm < 10mm was then added, followed by fine aggregate with grain size of 0-4.75 mm. The mix was given a quick stir for another 2 minutes. It was then poured into the oiled cast iron moulds, tapped for bubbles, and covered with plastic on the surface before placing it for curing (at room temperature and in oven) and left undisturbed for hardening.

Making of alkaline activating solution of desired molar ratio of SiO₂:Na₂O: The alkaline activating solution was made by adding sodium hydroxide pellets in measured commercial sodium silicate solution to achieve the desired molar ratio and then a measured quantity was taken for making the targeted trial mix. The alkaline activator solution was made 24 hrs. before use. The details of the calculation for making a molar ratio-specific activating solution are given in **Table 4**.

The solutions were prepared such that the sodium hydroxide pellets dissolved completely and the solution came to room temperature. They were stored in an air-tight blue cap Borosil bottle. All the measurements were done on a weight-by-weight basis.

Calculating and quantifying molar ratios: Moles of each element were calculated by first measuring the element-oxide in the desired precursor using X-ray Fluorescence

Spectroscopy (XRF). Then, the weight of element oxide in the weighed precursor sample was calculated in the following steps,

- i. Wt. of element oxide (g) = (weight of precursor (g) × percent of element oxide) / 100
- ii. Moles of element oxide = weight of element oxide as derived from (i) / molecular weight of that element oxide
- iii. Molar ratio of two element oxides = Moles of element oxide A / Moles of element oxide B

| Sample Code | Sample Composition | SiO ₂ :Na ₂ O Molar Ratio of Activating Alkaline Solution | SiO ₂ :Al ₂ O ₃ Molar Ratio of Mix | SiO ₂ :Na ₂ O Molar Ratio of Mix | Na ₂ O:Al ₂ O ₃ Molar Ratio of Mix | Binder: Aggregate: Coarse Aggregate Ratio (By Weight) | Fine (By | Curing Conditions |
|-------------|---------------------------------|---|---|--|---|---|----------|--|
| R1 | Calcined Sludge (600°C - 1 Hr.) | 2.00 | 4.57 | 4.41 | 1.04 | 1:1:2 | | Room temperature, oven 85°C for 1.5 hrs. |
| R2 | Calcined Sludge (700°C - 1 Hr.) | 2.00 | 4.60 | 4.43 | 1.04 | 1:1:2 | | Ambient room temperature |
| R3 | Calcined Sludge (600°C - 1 Hr.) | 2.00 | 4.10 | 5.13 | 0.80 | 1:1.5:3 | | Oven 85°C for 4 hrs. |
| R4 | Calcined Sludge (600°C - 1 Hr.) | 2.00 | 4.92 | 4.08 | 1.20 | 1:1.5:3 | | Oven 85°C 24 hrs. |
| R5 | Calcined Sludge (600°C - 1 Hr.) | 1.85 | 4.22 | 4.27 | 1.00 | 1:1.5:3 | | Oven 73°C 14 hrs. |
| R6 | Calcined Sludge (600°C - 1 Hr.) | 1.70 | 4.55 | 3.79 | 0.80 | 1:1.5:3 | | Oven 85°C 4 hrs. |
| R7 | Calcined Sludge (600°C - 1 Hr.) | 1.70 | 4.55 | 3.79 | 0.80 | 1:1.5:3 | | Oven 60°C 24 hrs. |
| R8 | Calcined Sludge (600°C - 1 Hr.) | 2.00 | 4.10 | 5.13 | 0.80 | 1:1.5:3 | | Oven 60°C 24 hrs. |
| R9 | Calcined Sludge (600°C - 1 Hr.) | 2.00 | 4.91 | 4.08 | 1.20 | 1:1.5:3 | | Oven 60°C 4 hrs. |

TABLE 3
Varying ranges of factors influencing the compressive strength of geopolymers

TABLE 4
Preparation of Alkaline Activating solution of desired molar ratios

| Alkaline Solution with Specific Molar Ratio (M.R) | Activating sodium silicate solution | Sodium Hydroxide Pellets to be added (weight basis) | Additional Na ₂ O (g) from NaOH pellet | Total SiO ₂ | Total Na ₂ O | Moles of SiO ₂ | Moles of Na ₂ O | M.R of SiO ₂ /Na ₂ O |
|---|-------------------------------------|---|---|------------------------|-------------------------|---------------------------|----------------------------|--|
| Units | | Percent | Percent | Percent | Percent | | | |
| Commercial Silicate solution | | 0.00 | 0.00 | 27.89 | 8.47 | 0.46 | 0.14 | 3.28 |
| M.R of 1.7 | | 10.9 | 8.45 | 27.89 | 16.92 | 0.46 | 0.27 | 1.70 |

| | | | | | | | |
|-------------|------|------|-------|-------|------|------|------|
| M.R of 1.85 | 9.10 | 7.05 | 27.89 | 15.52 | 0.46 | 0.25 | 1.85 |
| M.R of 2.0 | 7.60 | 5.89 | 27.89 | 14.36 | 0.46 | 0.23 | 2.00 |

If the weight of the precursor material was to be changed then the molar ratio of desired element oxides changed too. In Batch III, to achieve a Na: Al molar ratio of 1, the following formula was used:

$$\text{Wt. of Precursor (g)} = \frac{100 \text{ gm liquid silicate} \times A \% \text{ of sodium oxide in liquid} \times 101.96 \frac{\text{g}}{\text{mol}} \text{ of aluminium oxide}}{B \% \text{ of aluminium oxide in precursor material} \times 61.98 \frac{\text{g}}{\text{mol}} \text{ of sodium oxide}}$$

Source: (Davidovits, 2020)

The above calculation determines the weight of the precursor required in 100 gm of alkaline activating solution to achieve Na:Al molar ratio of the mix. Further variations of Na: Al were done, by entering all the values and formulas in Excel and varying the quantity of precursor until the desired Na: Al ratio was achieved in the output.

Characterization of hardened geopolymer specimens

Specimens were measured for their dimensions using a vernier calliper with a 0.01 cm least count. The weight of specimens was measured using a calibrated weighing balance. The specimens were tested for their compressive strength at the Structural Engineering laboratory. Furthermore, FTIR and SEM analysis of the samples were carried out to understand the influence of variable parameters on the geopolymer specimens. TCLP was carried out to understand the leachability of heavy metals from the geopolymer specimens using a Millipore Rotatory Agitator (Model Y132 ORA HW India) and the leachate was analysed on ICP OES (Model iCAP 6000 series).

Confirmatory tests for hardened geopolymer - The hardened geopolymers were subjected to additional tests of boiling water/steam and thermal dilatometry in the laboratory. In the Boiling water/steam test, the hardened geopolymers were put for 15 mins in boiling water at 100°C. It is one of the most severe tests that can be easily done in a single cycle. Specimens that are not fully condensed or with non-reactive ingredients disintegrate/deform completely during this experiment.

Thermal behaviour or Thermal dilatometry at 250°C: In this test, fully condensed geopolymer specimens are exposed to a temperature of 250°C for 30 mins using a muffle furnace (temperature ramping rate of 10°C/min). It is one of the sensitive tests for detecting uncondensed geopolymer specimens. Incompletely condensed geopolymer specimens undergo expansion, cracking, softening, and dehydration.

Statistical Analysis

The Design of Experiment (DOE) was designed using Minitab and the output (compressive strength) along with the independent variables (Na/Al molar ratio, curing temperature, curing time, molar ratio of SiO₂:Na₂O activating solution) was subjected to regression analysis. Pearson's coefficient of correlation was calculated for each independent and dependent variable.

III. RESULT AND DISCUSSION

Characterization of raw material and effects of calcination on sludge

The proximate analysis shows that the fresh sludge consists of 80-81% moisture while air-dried sludge contains only around 2-4% moisture content. The volatile solids in the sludge are about 20-22%, which could be due to the sediments from the raw water sources. The pH of water treatment plant sludge was in the neutral range while fly ash showed a pH in the basic range, as observed in **Table 5**. The particle size distribution test shows that the sludge primarily consists of silt and clay as shown in **Figure 1**. The nature of sludge is also influenced by the land use pattern surrounding the raw water source, as these contribute to the suspended solids in the water. The density of the sludge was calculated to be 1.04 g/cc while of fly ash was 1.35 g/cc.

TABLE 5
Physical Characteristics of water treatment plant sludge and fly ash

| Parameters | Units | Raw Sludge | Fly ash |
|-------------------------|---------|-------------|---------|
| pH | | 7.40 | 11.52 |
| Moisture content | Percent | 2.00-4.00 | < 1 |
| Volatile solids content | Percent | 20.00-22.00 | - |
| Ash content | Percent | 72.00-76.00 | - |

Note: ^aHeated at 105°C for 24 hrs. in oven, ^bCombustion at 550°C for 4 hrs., ^cFired at 1000°C for 2 hours.

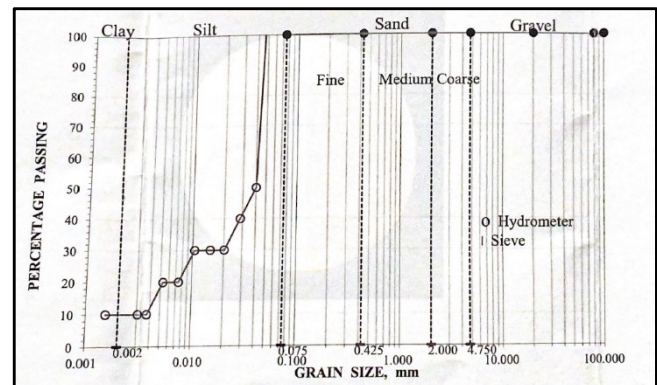


Figure 1: Particle Size Distribution of water treatment plant sludge

The CHNS content in the raw materials was estimated by LECO CHNS 628 and is given in **Table 6**. The raw sludge

contains total carbon in the range of 6.9-7.2%. This could be due to the influence of raw water characteristics, type of coagulant and dose, and factors like operating plant conditions while the fly ash shows low carbon content (Babatunde & Zhao, 2007). Calcination of sludge shows enhancement of pozzolanicity and reduction of carbon content.

TABLE 6
CHNS estimation of raw materials done by CHNS analyzer

| | Raw Sludge | Fly ash | Calcined sludge 600°C | Calcined sludge 700°C | Calcined sludge 800°C |
|----------------|------------|---------|-----------------------|-----------------------|-----------------------|
| Total carbon | 7.20 | 0.25 | 0.80 | 0.20 | 0.20 |
| Total Nitrogen | 0.72 | 0.13 | 0.16 | 0.03 | 0.06 |
| Total Hydrogen | 2.88 | 0.12 | 0.87 | 0.64 | 0.27 |

Note: All units are in percent (%)

Calcination of sludge: A Muffle furnace was used for performing the calcination of raw sludge. It was observed that increasing the thickness of the sludge in the ceramic crucibles for easier calcination caused the uppermost layer to oxidize while allowing the inner top layers to turn into amorphous carbon causing the surface to passivate and thereby preventing the sludge from oxidizing further (center remained uncalcined). Thus, inconsistency in the calcination process for sludge was observed and hence the method was improvised. From this point, the quantity of sludge was reduced and calcination was carried out in more batches with each crucible containing only about 2-3 mm thick sludge.

Table 7 illustrates the elemental composition of raw materials as determined by XRF. The raw water treatment plant sludge consists mainly of SiO₂, Al₂O₃, and small amounts of Fe₂O₃, MnO, CaO, MgO, and TiO₂. The sum of SiO₂, Al₂O₃, and Fe₂O₃ in raw and calcined sludge satisfies the criteria of pozzolana given by (IS:3812, 2013). Calcination at different temperatures improves the silica and alumina content slightly. XRF also reveals the presence of trace elements like oxides of Barium, gallium, vanadium, strontium, titanium, chromium, zinc, arsenic, and rubidium in addition to rare earth metals like yttrium oxide.

Pozzolanicity

The pozzolanicity of the raw materials was tested by performing the Modified Chapelle test. The amount of Calcium Hydroxide consumed was measured and the values are presented in **Figure 2**. The pozzolanic test findings show that the highest reactivity was observed in the calcined sludge at 600°C while the lowest reactivity was observed in fly ash followed by raw sludge. An increase in the calcination temperature of sludge shows a gradual reduction in the fixed

lime content indicating that rising temperature did not positively affect the reactivity of sludge. The French standard AFNOR NF P 18 – 513 and Brazilian Standard ABNT NBR 15894-1:(2010) state that the pozzolanic reactivity of a sample must not be lower than 750 mg Ca (OH)₂/g. (Ahmad et al., 2018) stated that calcination improvised the pozzolanic activity of the filter backwash solids and up to 20% replacement to cement complied with the IS specification for construction. (Tantawy, 2015) stated that calcination at higher temperatures affects the hydration of the material which in turn influences its reactivity with lime solution. Calcined sludge at 600°C showed promising performance as supplementary cementitious material as reported by (Godoy et al., 2020). (Messina et al., 2017) reported that properly condensed geopolymers could be obtained from poor natural waste subjected to calcination as it enhanced their mechanical properties.

TABLE 7
Elemental Composition of Raw Materials By XRF

| Elemental Composition XRF | Raw Sludge | FlyAsh | Calcined Sludge @600°C | Calcined Sludge @700°C | Calcined Sludge @800°C |
|--------------------------------|------------|--------|------------------------|------------------------|------------------------|
| SiO ₂ | 46.400 | 30.600 | 46.500 | 46.700 | 46.800 |
| Al ₂ O ₃ | 29.300 | 14.200 | 30.700 | 30.500 | 30.700 |
| Fe ₂ O ₃ | 14.100 | 17.200 | 13.200 | 13.200 | 13.100 |
| CaO | 2.010 | 22.500 | 1.940 | 1.950 | 1.940 |
| Na ₂ O | 0.371 | 2.310 | 0.350 | 0.336 | 0.370 |
| K ₂ O | 0.512 | 1.020 | 0.503 | 0.502 | 0.501 |
| MgO | 1.770 | 1.480 | 1.840 | 1.840 | 1.860 |
| P ₂ O ₅ | 0.752 | 0.177 | 0.727 | 0.721 | 0.723 |
| SO ₃ | 0.598 | 2.100 | 0.496 | 0.467 | 0.429 |
| Cl | 0.361 | 0.036 | 0.077 | 0.047 | 0.036 |
| TiO ₂ | 1.330 | 0.833 | 1.300 | 1.230 | 1.200 |
| V ₂ O ₅ | 0.051 | 0.029 | N.D | N.D | N.D |
| Cr ₂ O ₃ | 0.038 | ND | 0.039 | 0.035 | 0.041 |
| CuO | 0.028 | 0.010 | 0.024 | 0.023 | 0.022 |
| MnO | 2.270 | 0.218 | 2.160 | 2.160 | 2.120 |
| NiO | 0.025 | 0.018 | 0.021 | 0.015 | 0.019 |
| ZnO | 0.046 | 0.029 | 0.043 | 0.041 | 0.042 |
| Ga ₂ O ₃ | 0.004 | N.D | 0.006 | 0.006 | 0.005 |
| As ₂ O ₃ | 0.005 | 0.004 | N.D | N.D | N.D |
| Br | 0.016 | 0.002 | 0.004 | 0.002 | N.D |
| SrO | 0.015 | 0.076 | 0.013 | 0.012 | 0.013 |
| Y ₂ O ₃ | 0.004 | 0.004 | 0.004 | 0.004 | 0.003 |
| ZrO ₂ | 0.023 | 0.015 | 0.019 | 0.019 | 0.019 |
| Rb ₂ O | N.D | 0.004 | 0.004 | 0.002 | 0.004 |
| Co ₂ O ₃ | N.D | N.D | 0.009 | 0.018 | 0.009 |
| BaO | N.D | N.D | N.D | 0.078 | 0.068 |
| Total | 100.02 | 100.02 | 100.02 | 100.02 | 100.02 |

Note: ND- not detected; All values in weight percent

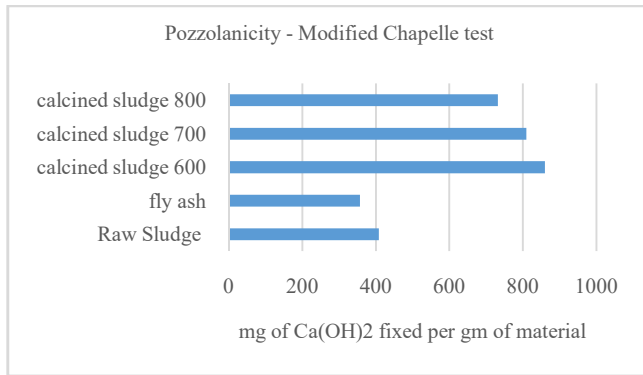


Figure 2: Pozzolanicity of Raw Materials

Total Organic Carbon

Carbon – in the inorganic and organic form was estimated in the raw materials by using TOC analyser. Highest percentage of organic carbon was observed in raw sludge as observed from **Figure 3**. Contribution of organic matter in the form of humic acid in the raw water source as well as addition of organic polymers during treatment processes can be one of the contributors of organic carbon in the sludge (Babatunde & Zhao, 2007). Calcined sludge shows low levels of total carbon when compared to its raw form. Calcination has helped in the removal of organic matter and the same is reflected by CHNS results too. Fly ash shows presence of organic carbon in very low quantities.

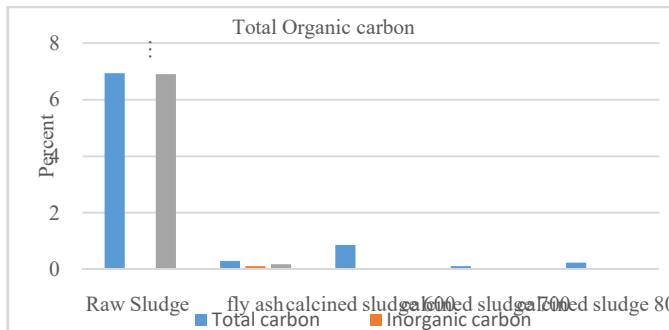
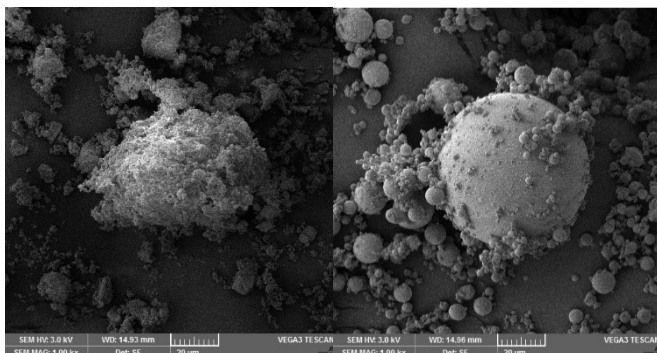


Figure 3: Total Organic carbon estimated by TOC analyzer

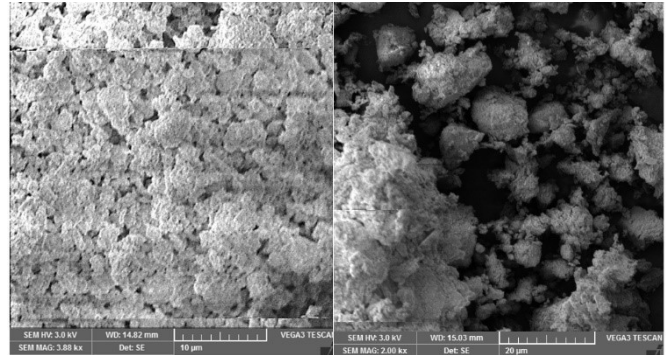
Scanning Electron Microscopy (SEM)

SEM was performed for the raw materials to understand the morphology of the particles. The SEM micrographs in **Figure 4** show that sludge is amorphous in nature and the particles are irregular in shape while fly ash particles are seen typically spherical in shape.



A) Raw Drinking Water Sludge

B) Fly Ash



C) Calcined Sludge at 600°C

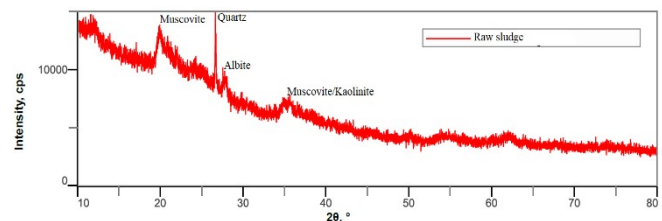
D) Calcined Sludge at 700°C

Figure 4: SEM Micrograph for: A) Raw Drinking Water Sludge, B) High Calcium Fly Ash, C) Calcined Sludge at 600°C, D) Calcined Sludge at 700°C

The sludge upon calcination shows variation in morphology. Sludge calcined at 600°C shows a change in particle shape to round and aggregated particles which are distinctive characteristics of the calcination process. A similar observation is seen for calcined sludge at 700°C where particles are seen to gather more closely than for calcined sludge at 600°C. A study conducted by (Godoy et al., 2020) shows similar behaviour of water treatment plant sludge on calcination at higher temperatures of 650°C and 750°C.

X-ray Diffraction (XRD)

The XRD diffractogram of the precursor materials is given in **Figure 5**. The x-ray powder diffraction pattern appears continuous for raw sludge indicating its amorphous nature. The peaks visible were identified to be quartz (Ferone et al., 2019; Godoy et al., 2020; Tantawy, 2015), albite (Ahmad et al., 2018; Tantawy, 2015) and Muscovite/kaolinite (Godoy et al., 2020; Suksiripattanapong, Horpibulsuk, Boongrasan, et al., 2015). XRD analysis for fly ash shows peaks identified as Quartz (Golek, 2019), Albite (Suksiripattanapong, Horpibulsuk, Chanprasert, et al., 2015), Hematite (Ziegler et al., 2016), Muscovite (Godoy et al., 2020) and MgO (Balakrishnan et al., 2020; Mings et al., 1983). Calcination of raw sludge at 600°C and 700°C for one hour each shows increased peak for quartz and albite while maintaining the amorphous nature of the sludge.



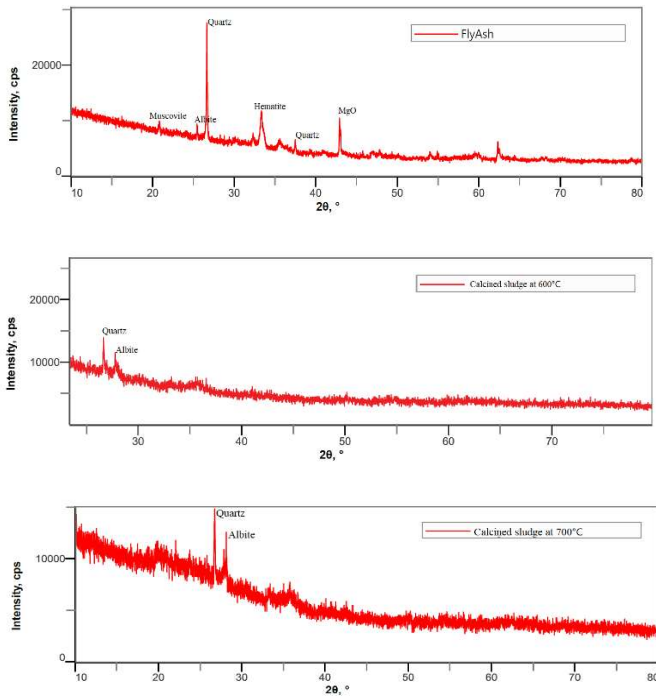


Figure 5: X-Ray Diffractogram of Raw Materials Used In The Study: (A) Raw Drinking Water Sludge; (B) Fly Ash; (C) Calcined Sludge At 600°C For 1 Hr; (D) Calcined Sludge At 700°C For 1 Hr

Mechanical properties of geopolymer pastes, mortars, and precast elements

The compressive strength for the geopolymer pastes and mortar for Batch I is given in **Figure 6**. The mixes for G1 to G5 failed to bear any load and cracked after being placed on the Universal Testing Machine for measurement of compressive strength. The poor load-bearing capacity could be attributed to the presence of carbon in the raw sludge, the lack of a proper method for mixing, and the varying physical ratios of sodium silicate and sodium hydroxide solutions that did not aid in the formation of bonds. These specimens were brittle and did not condense properly. However, geopolymer mortars of the G6 and G7 mix showed compressive strength in the range of 3.3 to 4.1 N/mm².

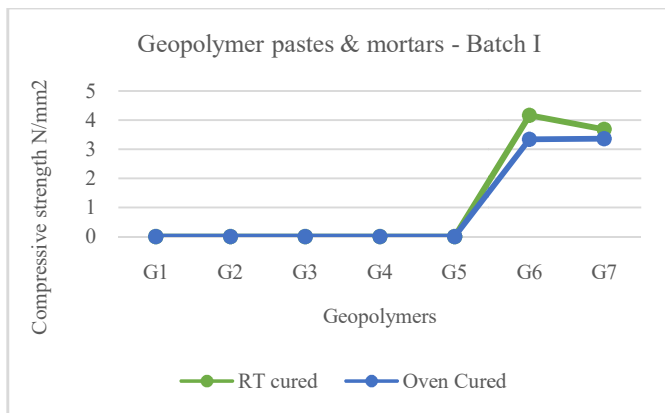


Figure 6: Compressive Strength For Batch I Geopolymer Paste and Mortar

The compressive strength obtained for Batch II is given in **Figure 7**. This batch had a SiO₂:Al₂O₃ molar ratio in a

variable range. M1 mix did not condense, instead turned into a mixture of powdery efflorescence and crumbled, and hence no compressive strength could be recorded. M2 mix condensed but behaved like a hygroscopic specimen that showed wetness on the surface. The cube was slippery and hence these two mixes were not considered for further investigation. M3 and M4 condensed and set very well. The cubes were dense and smooth with sharp edges, these were almost entirely made up of high calcium fly ash. These cubes show higher compressive strength of 4 to 14 N/mm².

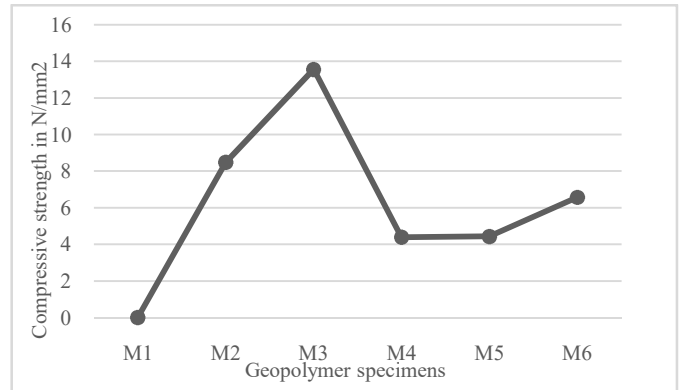


Figure 7: Compressive Strength Of Geopolymer With Varying SiO₂/Al₂O₃ Ratios

The results of compressive strength from Batch III are shown in **Figure 8**. Maximum compressive strength was reported for mix R6 with alkaline activating solution having a molar ratio of SiO₂:Na₂O of 1.7, Na₂O:Al₂O₃ molar ratio of the mix as 1.2, and curing temperature of 85°C for 4 hours.

The statistical analysis for Batch III shows a significant p-value (0.06) for Na/Al indicating that it affects the compressive strength of specimens. The other independent variables do not show any significant effect on the specimens. Pearson's coefficient of correlation shows a moderate correlation between the Na/Al molar ratio and the compressive strength of the specimens.

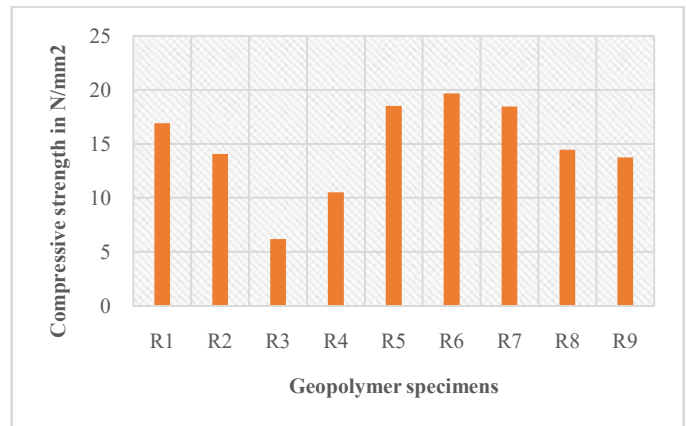


Figure 8: Compressive Strength of Geopolymer with varying Ranges of Influencing Factors

Effect of Attributes such as Water Content and Mixing Methods on Specimens

Water Content: Water was added to the geopolymer mix for better workability, however, it was observed that the addition of water affected the condensation process of the geopolymers. All the trials with additional water content did not set and the mixture remained wet even after 3-4 days of casting. They were discarded and the addition of water was avoided for further trials. Water does not get chemically bound in the geopolymerization process and acts as a diluting agent. The same mix was performed – with addition of water and without addition of water to understand its effect. The mix with extra water for workability did not condense and disintegrated after immersion in water, while the mix without any water addition, was fully condensed and did not collapse in water upon immersion.

Mixing method: The order of mixing the precursors, filler materials, and activating solution was carried out as shown in **Figure 9**.

It is important to proceed step-wise and in the manner that follows geopolymerization reaction kinetics. The main aluminosilicate precursor is usually the least reactive component and hence is added first to the alkaline activating solution. This mix is called the binder. The binder is mixed at optimized speed and time to allow depolymerization of silicates and allowed to rest. The consistency of the mix changes to gel-like post-aging and addition of most reactive components like ground blast furnace slag or inert components like sand & gravel are added to the mix. The mixture is then poured into the moulds, tapped to remove air/bubbles, and covered on top with waterproof plastic film to avoid loss of water due to evaporation before kept in the oven for curing. This is important as water acts as a medium to carry the cations in the silicate solution and oligo-sialates to become permanently attached in the aluminosilicate network (Davidovits, 2020).

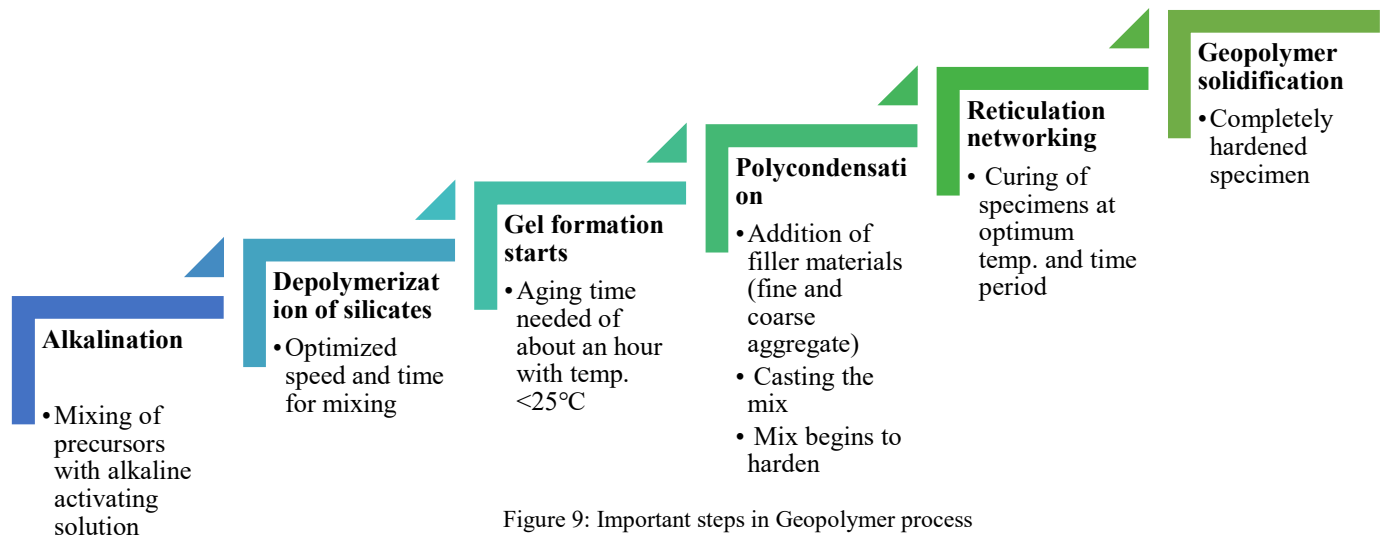


Figure 9: Important steps in Geopolymer process

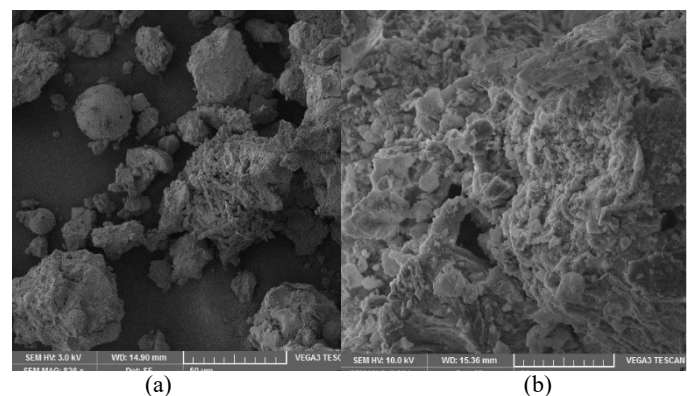
Characterization of Hardened Geopolymer Specimens

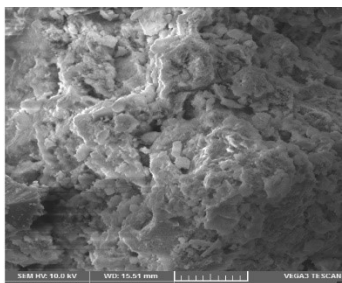
Scanning Electron Microscopy (SEM)

The condensed 28th-day cured geopolymer specimens show density in the range of 1.97 to 2.05 g/cc. Some of the specimens were selected for their microstructural analysis using SEM as seen in **Figure 10**.

From the SEM micrographs, a denser matrix can be seen for calcined sludge 600°C and 700°C geopolymers than fly ash geopolymers. Loose, unreacted fly ash particles can be in **Fig. 10a** indicating that not all fly ash particles participate in the geopolymerization process. The denser matrix indicates the development of proper geopolymer microstructure as seen in **Fig. 10b and 10c**. This demonstrates that calcination plays a very important role in improving the properties of a poor natural waste material. The calcined sludge geopolymer specimens with different curing temperatures show similar microstructure indicating that whilst temperature plays a vital

role in polycondensation reaction, the amorphous (pre-treated) precursors along with workable silicate solution (with optimum SiO₂:Na₂O molar ratio) is key in successfully achieving the geopolymerization process.





(c)

Figure 10: Microstructural Analysis of Condensed Geopolymer by SEM – (a) Fly Ash Geopolymer; (b) Calcined Sludge 600°C Geopolymer; (c) Calcined Sludge 700°C Geopolymer

Toxicity Characteristic Leaching Procedure (TCLP)

The TCLP analysis for the selected geopolymer specimens as shown in **Table 8** indicates that no detectable levels of heavy metals such as Chromium, Manganese, Zinc, Cadmium, Nickel, Cobalt, and Lead were observed in the leachates. However, higher values were observed for namely two metals - aluminium and iron in the specimens. As there are no EPA limits for these two metals, hence the specimens are acceptable as they show no detectable hazardous metal leaching behaviour.

TABLE 8
TCLP Results of Geopolymer Specimen

| Sr. No | Sample Code | Concentration Values (In ppb) | |
|--------|-------------|-------------------------------|-----------|
| | | Aluminium (Al) | Iron (Fe) |
| 1. | M3 | 1.83 | 0.701 |
| 2. | M4 | 0.463 | 0.167 |
| 3. | R5 | 0.733 | 0.459 |
| 4. | R6 | 1.12 | 1.02 |
| 5. | R7 | 19.6 | 15.7 |
| 6. | R1 | 1.03 | 0.535 |
| 7. | R2 | 0.47 | 1.3 |

Fourier Transform Infrared Spectroscopy (FTIR)

The presence of geopolymer structure can be confirmed by the FTIR spectra measurements as shown in **Fig. 11-15**. The absorption spectra of FTIR can be divided into groups of bands associated with the following:

- The vibration bands at 3680, 3436, 3388, 1636, 1628, 3458, and 1640-42 cm^{-1} are attributed to the presence of OH group and bending vibrations of water molecules. (Tantawy, 2015; Wajjarean et al., 2014)
- While the vibrations of O-C-O group are in the range of 1500-1400 cm^{-1} and at about 867 cm^{-1} (Hasnaoui et al., 2019; Król et al., 2016)
- Internal Si-O-Si and Si-O-Al bond vibration occur at 600-800 cm^{-1} , 1020-1000 cm^{-1} and 1200-400 cm^{-1} (Ferone et al., 2019)

Based on the FTIR spectra obtained of the geopolymer samples, the presence of bands at 3450, 3462, 3463, 3467 and 3557 cm^{-1} and at 1648, 1659 cm^{-1} can be attributed to the stretching and bending vibrations of OH group similar to the findings reported by (Wajjarean et al., 2014). The OH group in the aluminosilicates is contributed by water in the sodium silicate and sodium hydroxide components and thus confirm the presence of hydrated aluminosilicates in the resulting samples.

The absorption bands observed at 1422, 1459, 1460, 1462 and 1457 cm^{-1} and weak band at 851 cm^{-1} refer to the asymmetrical stretching of C-O bond of carbonates in sodium carbonates, as the reactant product of sodium hydroxide with atmospheric CO_2 as reported by (Król et al., 2016). Other bands in these spectra were seen at 1431 and 1373 cm^{-1} .

All the samples show the strongest vibration for Si-O-Si and Si-O-Al and Al-O-Si in the range of 458 – 468 cm^{-1} , 778-787 cm^{-1} , 1024-1039 cm^{-1} and 579-592 cm^{-1} that belong to typical aluminosilicate framework as confirmed by (Ferone et al., 2019). The in-plane bending vibration of Si-O-Si can be associated with the 458-468 cm^{-1} band while the 4 coordinated Al-O stretching vibration can be associated with the bands at 778-787 cm^{-1} . Bands at 592, 579 and 851 cm^{-1} can be assigned to the bending vibration of Al-O-Si bonds while the most prominent band at 1024-1039 cm^{-1} can be assigned to asymmetric stretching of the aluminosilicate species of Si-O-Al, Si-O-Si bond and verify the geopolymerization reaction as reported by (Catauro et al., 2015; Davidovits, 2020).

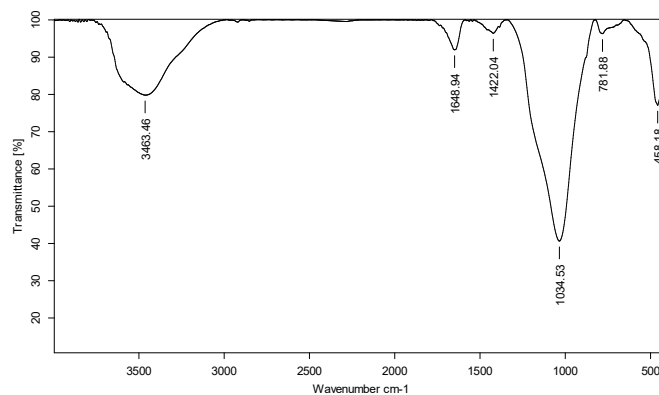


Figure 11: R5 Geopolymer FTIR Spectra

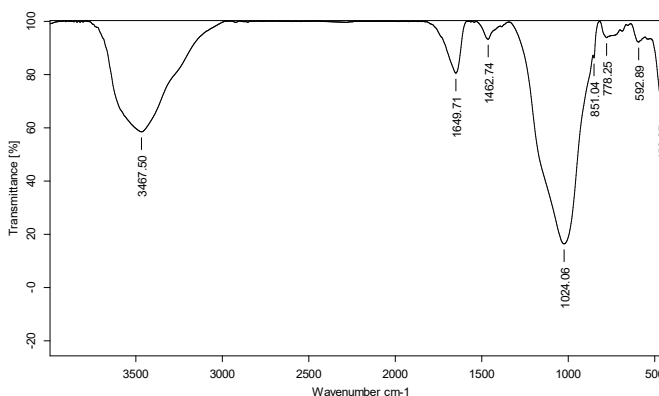


Figure 12: R6 Geopolymer FTIR Spectra

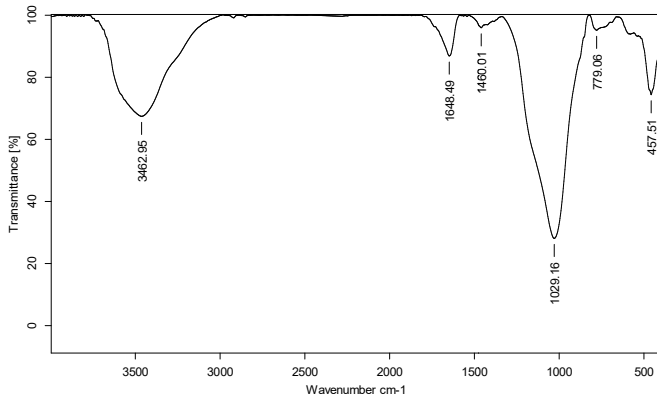


Figure 13: R7 Geopolymer FTIR Spectra

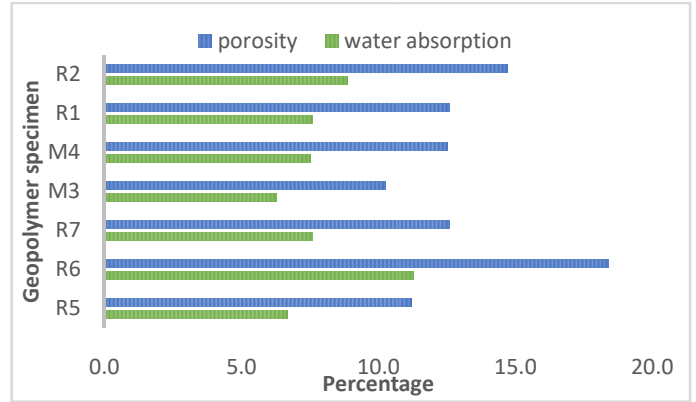


Fig. 16: Water Absorption and Porosity Of Selected Geopolymers

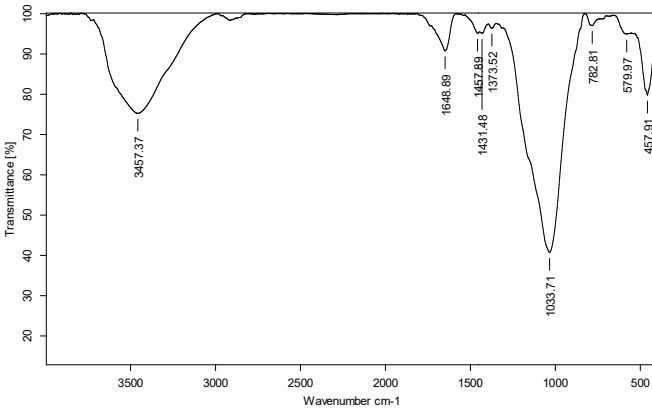


Figure 14: R1 Geopolymer FTIR Spectra

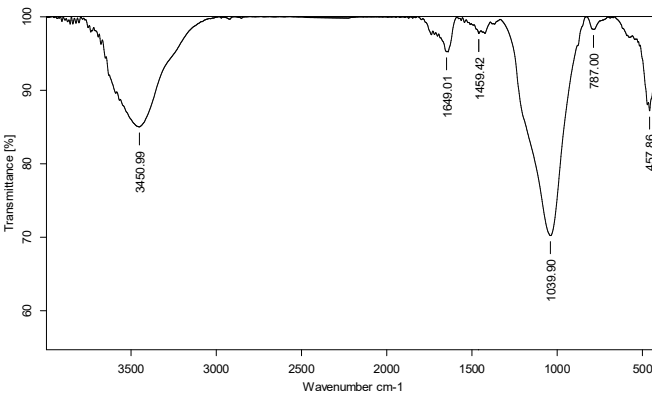


Figure 15: R2 Geopolymer FTIR Spectra

Confirmatory Tests For Geopolymers

The boiling water test is one the most severe tests that a chemically stable geopolymer can withstand without any distortion in shape or size. The geopolymer samples with the correct chemical formula showed stability and no change was observed in their structure after subjecting them to the boiling water test and thermal dilatometry test as shown in **Fig. 17 & 18**. It is evident from **Fig. 17 b and c**, that some of the samples show leaching (beaker no. 2 & 3) and were not stable while the sample in beaker no. 1 shows no change in the water, thus indicating it is chemically more stable. TCLP tests conducted do not show any detectable heavy metal leaching, indicating that samples are non-toxic. The leaching observed in the two beakers seen in Fig. 17 b & c could be due to the presence of other compounds in the sludge.

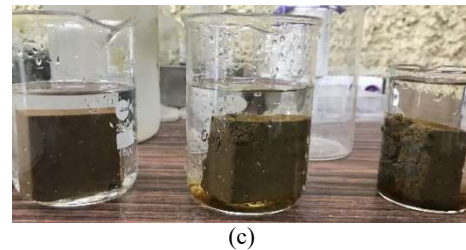
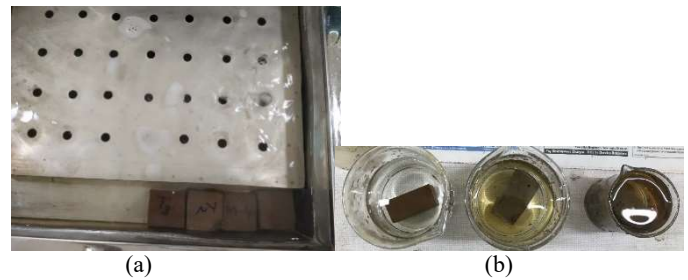


Fig. 17 Boiling Water Test

Water Absorption, Porosity and Density

The geopolymer specimen shows water absorption in the range of 6.3 to 14.8% and is given in **Fig. 16**. If these specimens are compared with the traditional burnt clay bricks which allows max. water absorption of 20% by weight upto class 12.5, these specimens are very well within the acceptable limit (IS 1077, 1992). The geopolymer specimen shows porosity varying from 10 to 19%. Specimens showing higher water absorption also showed higher values for porosity indicating that they are directly proportional.

In another confirmatory test of thermal dilatometry, the geopolymer specimens showed no expansion, cracks or distortion after being subjected to heating up to 250°C for 30 mins as seen in **Fig. 18**.

There are few studies that have used water treatment plant sludge as a precursor material for obtaining geopolymer

blocks. It is seen that calcination of sludge improves the availability of aluminium during the geopolymerization reaction which results in lesser setting time and better compressive strength (Najafi Kani et al., 2012). The results obtained in this study are in the same league and have been summarized in **Table 9**.

TABLE 9
Literature Review on Studies with Geopolymers from Water Treatment Plant Sludge

| Sr. No | Water Treatment Plant Sludge Use As | Activator | Molar Ratio | | Pre-Treatment Of Sludge | Curing Conditions | Compressive Strength | Ref. |
|--------|-------------------------------------|---|---|---|---------------------------------------|---|----------------------|--|
| | | | SiO ₂ /Al ₂ O ₃ Of Total Mix | Na ₂ O/SiO ₂ Of Activator Soln. | | | | |
| 1 | Precursor | Sodium hydroxide solution | 1.78 | 0.25 | Calcining at 600, 800,900°C for 1 hr. | Ambient 28°C for 24 hrs. | 1-8 MPa | (Waijarean et al., 2014) |
| 2 | Precursor | Sodium silicate solution | 2.03 | 0.5 | Calcination at 650°C for 1 hr. | 25°C for 7 days and 60°C for 7 days | 3.9-16.64 MPa | (Ferone et al., 2019) |
| 3 | Precursor | Sodium silicate (SS) (R=3.2) and sodium hydroxide (SH) solution (14M) | 4.25 | Mass ratio of SS to SH is 2.32 | Calcination at 750°C for 2 hrs. | 20°C and 60°C for first 24 hrs. and then at 20°C for 28 days | 16.9-22 MPa | (Messina et al., 2017) |
| 4 | Aggregate | Sodium silicate solution, Sodium hydroxide solution | Not given | Mass ratio of SS to SH is 80:20 | - | 65°C for 24, 48, 72, 96 and 120 hrs. | 5-20 MPa | (Suksiripattanapong, Horpibulsuk, Boongrasan, et al., 2015) |
| 5 | Precursor | Potassium hydroxide, Potassium silicate | 2.06-3.73 | Not given | Calcination at 750°C for 6 hrs. | Ambient temperature | 22-89 MPa | (Santos et al., 2019) |
| 6 | Precursor | Sodium silicate solution, Sodium hydroxide solution | 4.9-5.9 | Mass ratio of SS to SH is 1.5 | Calcination at 600°C for 2 hrs. | Room temperature and 60°C | ~19 MPa | (Nimwinya et al., 2016) |
| 7 | Aggregate | Sodium silicate solution, Sodium hydroxide solution (10M) | Not given | Mass ratio of SS to SH is 80:20 | - | Curing at 65, 75 and 85 °C respectively for durations of 24, 48, 72, 96 and 120 h | 12-20 MPa | (Suksiripattanapong, Horpibulsuk, Chanprasert, et al., 2015) |

Note: $R = SiO_2:Na_2O$ molar ratio



(i)



(ii)



(iii)

Fig. 18 Thermal Dilatometry Test –

- (i) Before Subjecting To 250°C;
- (ii) After Subjecting To 250°C;
- (iii) Sample Kept In A Muffle Furnace For Thermal Dilatometry Test

IV. CONCLUSIONS

In this study, the recycling of water treatment plant sludge and high calcium fly ash as geopolymeric precursors was explored. The study was conducted through a series of steps which included initial characterization of raw materials and their calcination to further upscaling the process to achieve the desired outcome. Calcination of water treatment plant sludge at 600°C for 1 hour was considered the optimum pre-treatment in this study as it showed the highest pozzolanicity by the Modified Chapelle test. The SEM micrographs along with FTIR spectra of the specimen confirms the presence of crystalline reaction products mainly – Sodium alumino-silicate hydrate gel. The prepared geopolymer specimens show the highest compressive strength of ~20 MPa after 28 days. There is nodetectable heavy metal leaching from the developed geopolymer blocks as confirmed by TCLP rendering them safe for implementation. The samples did not show any change post-water immersion for 15 days. The water absorption and porosity of the blocks were measured and found to be in the range of 6-14% and 10-19%, respectively.

The results obtained from this research can provide a practical reference in understanding the molar ratios and curing conditions to design and optimise geopolymeric compositions entirely from aluminosilicate-rich waste materials. Although the proposed research work suggests that using alumino-silicate-rich wastes can be suitable for producing construction products/materials, more technical investigation is required to improve the mechanical properties of the specimen. Further studies to investigate the setting time, durability, workability, thermal conductivity, and permeability of the specimens from an environmental perspective can be done to assess the performance of the blocks. Recycling drinking water sludge and fly ash can reduce the storage space required in lagoons and landfills.

The geopolymerization process is one of the green methods for developing construction products with lesser carbon dioxide emission compared to ordinary Portland cement. The geopolymeric blocks obtained can be used for the application of non-structural purposes such as:

- a. Replacement to paver blocks/bricks in pavement works
- b. As a unit for constructing boundary walls for gardens or fences
- c. Jogging tracks, walking paths for lightweight traffic in parks/gardens
- d. As filler materials in the construction of roads, or also as embankments

V. ACKNOWLEDGEMENT

The authors are grateful to CSIR-NEERI for providing infrastructure facilities, AcSIR-NEERI, and CSIR HRDG (for Direct-SRF Fellowship) for financial support. The author is grateful to DST and SAIF/CRNTS, IIT Bombay for providing XRF and FTIR analytical facilities for the research work and VJTI, Matunga for providing facilities to carry out mechanical tests. The authors gratefully acknowledge the support provided by the Director, CSIR-NEERI.

Declaration of Competing Interest

The authors declare that they have no conflict of interest.

VI. REFERENCES

- Ahmad, T., Ahmad, K., & Alam, M. (2017). Sludge quantification at water treatment plant and its management scenario. *Environmental Monitoring and Assessment*, 189(9). <https://doi.org/10.1007/s10661-017-6166-1>
- Ahmad, T., Ahmad, K., & Alam, M. (2018). Investigating calcined filter backwash solids as supplementary cementitious material for recycling in construction practices. *Construction and Building Materials*, 175, 664–671. <https://doi.org/10.1016/j.conbuildmat.2018.04.227>
- Babatunde, A. O., & Zhao, Y. Q. (2007). Constructive approaches toward water treatment works sludge management: An international review of beneficial reuses. In *Critical Reviews in Environmental Science and Technology* (Vol. 37, Issue 2, pp. 129–164). <https://doi.org/10.1080/10643380600776239>
- Balakrishnan, G., Velavan, R., Mujasam Batoo, K., & Raslan, E. H. (2020). Microstructure, optical and photocatalytic properties of MgO nanoparticles. *Results in Physics*, 16(November 2019), 103013. <https://doi.org/10.1016/j.rinp.2020.103013>
- Catauro, M., Papale, F., Lamanna, G., & Bollino, F. (2015). Geopolymer/PEG hybrid materials synthesis and investigation of the polymer influence on microstructure and mechanical behavior. *Materials Research*, 18(4), 698–705. <https://doi.org/10.1590/1516-1439.342814>
- Chen, H. X., Ma, X., & Dai, H. J. (2010). Reuse of water purification sludge as raw material in cement production. *Cement and Concrete Composites*, 32(6), 436–439. <https://doi.org/10.1016/J.CEMCONCOMP.2010.02.009>
- Cong, P., & Cheng, Y. (2021). Advances in geopolymer materials: A comprehensive review. *Journal of Traffic and Transportation Engineering (English Edition)*, 8(3), 283–314. <https://doi.org/10.1016/j.jtte.2021.03.004>
- Davidovits, J. (2017). Geopolymers: Ceramic-like inorganic

- polymers. *Journal of Ceramic Science and Technology*, 8(3), 335–350. <https://doi.org/10.4416/JCST2017-00038>
- Davidovits, J. (2020). *Geopolymer Chemistry and Applications* (Vol. 171).
- Davidovits, J., Izquierdo, M., Querol, X., Antenucci, D., Nugteren, H., Butselaar-Orthlieb, V., Fernández-Pereira, C., & Luna, Y. (2008). The European research project geoash: Geopolymeric cement based on European fly-ashes. *A Global Road Map for Ceramic Materials and Technologies: Forecasting the Future of Ceramics, International Ceramic Federation - 2nd International Congress on Ceramics, ICC 2008, Final Programme*, 4(0), 0–10.
- El-Didamony, H., Khalil, K. A., & Heikal, M. (2014). Physico-chemical and surface characteristics of some granulated slag-fired drinking water sludge composite cement pastes. *HBRC Journal*, 10(1), 73–81. <https://doi.org/10.1016/j.hbrcj.2013.09.004>
- Fang, X., Wang, L., Poon, C. S., Baek, K., Tsang, D. C. W., & Kwok, S. K. (2019). Transforming waterworks sludge into controlled low-strength material: Bench-scale optimization and field test validation. *Journal of Environmental Management*, 232, 254–263. <https://doi.org/10.1016/j.jenvman.2018.11.091>
- Ferone, C., Capasso, I., Bonati, A., Roviello, G., Montagnaro, F., Santoro, L., Turco, R., & Cioffi, R. (2019). Sustainable management of water potabilization sludge by means of geopolymers production. *Journal of Cleaner Production*, 229, 1–9. <https://doi.org/10.1016/j.jclepro.2019.04.299>
- Godoy, L. G. G. de, Rohden, A. B., Garcez, M. R., Da Dalt, S., & Bonan Gomes, L. (2020). Production of supplementary cementitious material as a sustainable management strategy for water treatment sludge waste. *Case Studies in Construction Materials*, 12. <https://doi.org/10.1016/j.cscm.2020.e00329>
- Golek, Ł. (2019). Glass powder and high-calcium fly ash based binders – Long term examinations. *Journal of Cleaner Production*, 220, 493–506. <https://doi.org/10.1016/j.jclepro.2019.02.095>
- Gress, D. 1997. *Early Distress of Concrete Pavements*, Report No. FHWA-SA-97-045. Federal Highway Administration, Washington, DC.
- Hasnaoui, A., Ghorbel, E., & Wardeh, G. (2019). Optimization approach of granulated blast furnace slag and metakaolin based geopolymer mortars. *Construction and Building Materials*, 198, 10–26. <https://doi.org/10.1016/j.conbuildmat.2018.11.251>
- Horpibulsuk, S., Suksiripattanapong, C., Samingthong, W., Rachan, R., & Arulrajah, A. (2016). Durability against Wetting–Drying Cycles of Water Treatment Sludge–Fly Ash Geopolymer and Water Treatment Sludge–Cement and Silty Clay–Cement Systems. *Journal of Materials in Civil Engineering*, 28(1), 04015078. [https://doi.org/10.1061/\(asce\)mt.1943-5533.0001351](https://doi.org/10.1061/(asce)mt.1943-5533.0001351)
- Horth, H., Gendebien, A., Agg, R. and Cartwright, N. (1994). Treatment and disposal of waterworks sludge in selected European countries. In: Foundation for water research technical reports No.FR 0428.
- Huang, C. H., & Wang, S. Y. (2013). Application of water treatment sludge in the manufacturing of lightweight aggregate. *Construction and Building Materials*, 43, 174–183. <https://doi.org/10.1016/J.CONBUILDMAT.2013.02.016>
- Huang, C., Pan, J. R., & Liu, Y. (2005). Mixing Water Treatment Residual with Excavation Waste Soil in Brick and Artificial Aggregate Making. *Journal of Environmental Engineering*, 131(2), 272–277. [https://doi.org/10.1061/\(asce\)0733-9372\(2005\)131:2\(272\)](https://doi.org/10.1061/(asce)0733-9372(2005)131:2(272))
- Huang, C., Pan, J. R., Sun, K.-D., & Liaw, C.-T. (2001). Reuse of water treatment plant sludge and dam sediment in brick-making. *Water Science and Technology*, 44(10), 273–277. <https://doi.org/10.2166/wst.2001.0639>
- Iribarne, J. V, Iribarne, A. P., Blondin, J., & Anthony, E. J. (2001). Hydration of combustion ashes — a chemical and physical study. *Fuel*, 80, 773–784.
- IS:3812. (2013). Specification for Pulverized fuel ash, Part-1: For Use as Pozzolana in Cement, Cement Mortar and Concrete. *Bureau of Indian Standards, New Delhi, India*, 1–12.
- IS 1077. (1992). Building Common Burnt Clay Building Bricks- Specificatins. *Bureau of Indian Standard(BIS)*.
- Keeley, J., Jarvis, P., & Judd, S. J. (2014). Coagulant recovery from water treatment residuals: A review of applicable technologies. *Critical Reviews in Environmental Science and Technology*, 44(24), 2675–2719. <https://doi.org/10.1080/10643389.2013.829766>
- Kiziniėvič, O., Žurauskienė, R., Kiziniėvič, V., & Žurauskas, R. (2013). Utilisation of sludge waste from water treatment for ceramic products. *Construction and Building Materials*, 41, 464–473. <https://doi.org/10.1016/J.CONBUILDMAT.2012.12.041>
- Król, M., Minkiewicz, J., & Mozgawa, W. (2016). IR spectroscopy studies of zeolites in geopolymeric materials derived from kaolinite. *Journal of Molecular Structure*, 1126, 200–206. <https://doi.org/10.1016/j.molstruc.2016.02.027>
- Mahmoodi, O., Siad, H., Lachemi, M., Dadsetan, S., & Sahmaran, M. (2020). Optimization of brick waste-based geopolymer binders at ambient temperature and pre-targeted chemical parameters. *Journal of Cleaner*

- Production*, 268.
<https://doi.org/10.1016/j.jclepro.2020.122285>
- Messina, F., Ferone, C., Molino, A., Roviello, G., Colangelo, F., Molino, B., & Cioffi, R. (2017). Synergistic recycling of calcined clayey sediments and water potabilization sludge as geopolymer precursors: Upscaling from binders to precast paving cement-free bricks. *Construction and Building Materials*, 133, 14–26. <https://doi.org/10.1016/j.conbuildmat.2016.12.039>
- Mings, M. L., Schlorholtz, S. M., Pitt, J. M., & Demirel, T. (1983). Characterization of Fly Ash By X-Ray Analysis Methods. *Transportation Research Record*, 5–11.
- Mohapatra, R., & Rao, J. R. (2001). Some aspects of characterisation, utilisation and environmental effects of fly ash. *Journal of Chemical Technology & Biotechnology*, 76(1), 9–26. [https://doi.org/https://doi.org/10.1002/1097-4660\(200101\)76:1<9::AID-JCTB335>3.0.CO;2-5](https://doi.org/https://doi.org/10.1002/1097-4660(200101)76:1<9::AID-JCTB335>3.0.CO;2-5)
- Monteiro, S. N., Alexandre, J., Margem, J. I., Sánchez, R., & Vieira, C. M. F. (2008). Incorporation of sludge waste from water treatment plant into red ceramic. *Construction and Building Materials*, 22(6), 1281–1287. <https://doi.org/10.1016/j.conbuildmat.2007.01.013>
- Mudgal, M., Singh, A., Chouhan, R. K., Acharya, A., & Srivastava, A. K. (2021). Fly ash red mud geopolymer with improved mechanical strength. *Cleaner Engineering and Technology*, 4, 100215. <https://doi.org/10.1016/J.CLET.2021.100215>
- Najafi Kani, E., Allahverdi, A., & Provis, J. L. (2012). Efflorescence control in geopolymer binders based on natural pozzolan. *Cement and Concrete Composites*, 34(1), 25–33. <https://doi.org/10.1016/J.CEMCONCOMP.2011.07.007>
- Nimwinya, E., Arjarn, W., Horpibulsuk, S., Phoo-Ngernkham, T., & Poowancum, A. (2016). A sustainable calcined water treatment sludge and rice husk ash geopolymer. *Journal of Cleaner Production*, 119, 128–134. <https://doi.org/10.1016/j.jclepro.2016.01.060>
- Pan, R., Huang, C., & Lin, S. (2004). Reuse of fresh water sludge in cement making. *Water Science and Technology: A Journal of the International Association on Water Pollution Research*, 50(9), 183–188.
- Ren, D., Yan, C., Duan, P., Zhang, Z., Li, L., & Yan, Z. (2017). Durability performances of wollastonite, tremolite and basalt fiber-reinforced metakaolin geopolymer composites under sulfate and chloride attack. *Construction and Building Materials*, 134(C), 56–66. <https://doi.org/10.1016/j.conbuildmat.2016.12.103>
- Sales, A., De Souza, F. R., & Almeida, F. D. C. R. (2011). Mechanical properties of concrete produced with a composite of water treatment sludge and sawdust. *Construction and Building Materials*, 25(6), 2793–2798. <https://doi.org/10.1016/J.CONBUILDMAT.2010.12.057>
- Santos, G. Z. B., Melo Filho, J. A., Pinheiro, M., & Manzato, L. (2019). Synthesis of water treatment sludge ash-based geopolymers in an Amazonian context. *Journal of Environmental Management*, 249. <https://doi.org/10.1016/j.jenvman.2019.109328>
- Suksiripattanapong, C., Horpibulsuk, S., Boongrasan, S., Udomchai, A., Chinkulkijniwat, A., & Arulrajah, A. (2015). Unit weight, strength and microstructure of a water treatment sludge-fly ash lightweight cellular geopolymer. *Construction and Building Materials*, 94, 807–816. <https://doi.org/10.1016/j.conbuildmat.2015.07.091>
- Suksiripattanapong, C., Horpibulsuk, S., Chanprasert, P., Sukmak, P., & Arulrajah, A. (2015). Compressive strength development in fly ash geopolymer masonry units manufactured from water treatment sludge. *Construction and Building Materials*, 82, 20–30. <https://doi.org/10.1016/j.conbuildmat.2015.02.040>
- Tang, C. W., & Cheng, C. K. (2019). Partial replacement of fine aggregate using water purification sludge in producing CLSM. *Sustainability (Switzerland)*, 11(5). <https://doi.org/10.3390/su11051351>
- Tantawy, M. A. (2015). Characterization and pozzolanic properties of calcined alum sludge. *Materials Research Bulletin*, 61, 415–421. <https://doi.org/10.1016/j.materresbull.2014.10.042>
- Teixeira, S. R., Santos, G. T. A., Souza, A. E., Alessio, P., Souza, S. A., & Souza, N. R. (2011). The effect of incorporation of a Brazilian water treatment plant sludge on the properties of ceramic materials. *Applied Clay Science*, 53(4), 561–565. <https://doi.org/10.1016/J.CLAY.2011.05.004>
- Tishmack, J. K., Olek, J., & Diamond, S. (1999). Characterization of high-calcium fly ashes and their potential influence on ettringite formation in cementitious systems. *Cement, Concrete and Aggregates*, 21(1), 82–92. <https://doi.org/10.1520/cca10512j>
- Waijarean, N., Asavapisit, S., & Sombatsompop, K. (2014). Strength and microstructure of water treatment residue-based geopolymers containing heavy metals. *Construction and Building Materials*, 50, 486–491. <https://doi.org/10.1016/j.conbuildmat.2013.08.047>
- Yao, Z. T., Ji, X. S., Sarker, P. K., Tang, J. H., Ge, L. Q., Xia, M. S., & Xi, Y. Q. (2015). A comprehensive review on the applications of coal fly ash. *Earth-Science Reviews*, 141, 105–121. <https://doi.org/10.1016/j.earscirev.2014.11.016>
- Ziegler, D., Formia, A., Tulliani, J. M., & Palmero, P. (2016).

Environmentally-friendly dense and porous geopolymers using fly ash and rice husk ash as raw materials. *Materials*, 9(6). <https://doi.org/10.3390/ma9060466>